Computer Aided Geometric Design 35–36 (2015) 225–242

Contents lists available at ScienceDirect

Computer Aided Geometric Design

www.elsevier.com/locate/cagd

On extraordinary rules of quad-based interpolatory subdivision schemes

Paola Novara [a,*], Lucia Romani [b]

[a] Dipartimento di Scienza e Alta Tecnologia, Università dell'Insubria, Via Valleggio 11, 22100 Como, Italy
[b] Dipartimento di Matematica e Applicazioni, Università di Milano-Bicocca, Via R. Cozzi 55, 20125 Milano, Italy

ARTICLE INFO

Article history:
Available online 23 March 2015

Keywords:
Subdivision schemes
Interpolation
Extraordinary vertices
C^1 continuity
Bounded curvature

ABSTRACT

This article deals with interpolatory subdivision schemes generalizing the tensor-product version of the Dubuc–Deslauriers 4-point scheme to quadrilateral meshes of arbitrary manifold topology. In particular, we focus our attention on an extension of the C^1 regular stencils that respectively exploits $(N+2)$-point and $(2N+8)$-point stencils for the computation of an edge-point and a face-point in the vicinity of an extraordinary vertex of valence $N \neq 4$ not lying on a boundary. The aim of our work consists in identifying which constraints are required to be respected by the weights appearing in the above stencils in order to get closed limit surfaces that are C^1-continuous at extraordinary points, have both principal curvatures bounded and at least one of them nonzero. The obtained constraints are used to easily check these features in the limit surfaces resulting from the application of special extraordinary rules proposed in the literature by different authors. Moreover, the conditions derived on the stencil weights are exploited to design new extraordinary rules that can produce closed limit surfaces of the same quality as the existing proposals, but at a reduced computational cost.

1. Introduction

Subdivision schemes are computationally efficient algorithms for representing smooth surfaces by applying a few steps of a refinement operator to a given polygonal mesh, roughly describing the desired limit shape. Each application of the refinement operator aims at splitting the edges and faces of the current mesh to obtain a finer and smoother version. Compared with parametric surface representations, subdivision schemes are no longer restricted to work with tensor-product meshes, but can advantageously operate on polygonal meshes of arbitrary manifold topology in order to generate surfaces of arbitrary topology. Polygonal meshes consisting entirely of quadrilateral faces are called quadrilateral meshes. Using the term *valence* to refer to the number of edges incident to a vertex, we have that, in case of quadrilateral meshes, all vertices of valence 4 are *regular* or *ordinary*, whereas vertices of valence other than 4 are *extraordinary*. In case of quadrilateral meshes, the refinement operator responsible for producing the finer mesh from the coarser one is specified by a set of topological and geometrical rules that can vary according to the properties that the limit surface is required to satisfy. More precisely, if the limit surface is required to pass through all the vertices of the given initial mesh, then the refinement operator relies upon topological rules that retain the vertices of the coarser mesh and insert new vertices in correspondence to the midpoint of its edges and the centroid of its faces. Such vertices are respectively called *edge-points* and *face-points*, and are

* Corresponding author.
E-mail addresses: paola.novara@uninsubria.it (P. Novara), lucia.romani@unimib.it (L. Romani).

http://dx.doi.org/10.1016/j.cagd.2015.03.018
0167-8396/

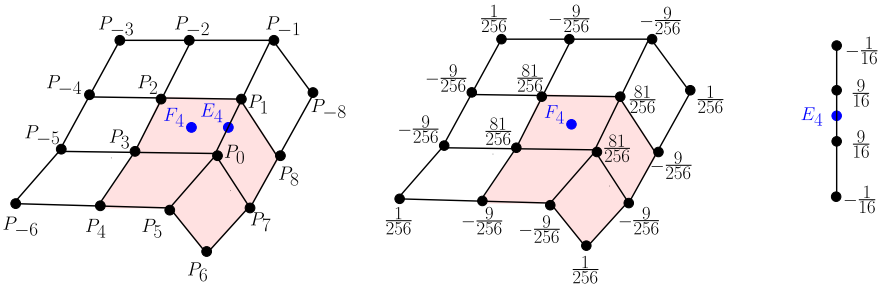

Fig. 1. Edge-point and face-point rules for regular regions.

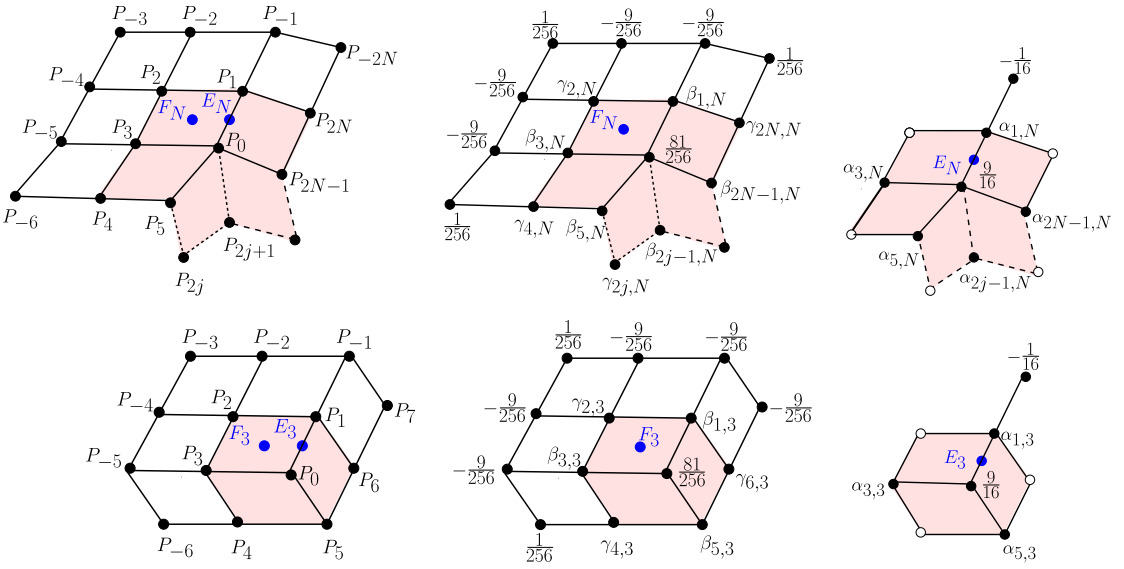

Fig. 2. Edge-point and face-point rules in the neighborhood of extraordinary vertices of valence $N \geq 5$ (top) and $N = 3$ (bottom).

hereinafter denoted by E and F (see Figs. 1, 2). A refined mesh is then obtained by constructing new edges and faces in the following way: first, we create all new edges of the refined mesh by connecting each face-point to the edge-points of the edges surrounding the face, and each mesh vertex to the edge-points of the edges incident on it; then, all new faces are simply obtained by the loop of four new edges. The role of the geometrical rules is instead to specify the positions of the new points. Edge-point and face-point rules consist in computing affine combinations of the vertices lying in the neighborhood of each edge or face of the coarser mesh. The choice of the weights to be used in the affine combination has been always considered a difficult problem. In fact, in order to maximize the global smoothness of the limit surface it is necessary to apply special edge- and face-point rules in the neighborhood of all extraordinary vertices. Such rules, besides being expected to be dependent on the valence of the extraordinary vertex, should involve the least possible number of control points in its vicinity in order to increase the locality of the scheme and consequently reduce the computational cost of each refinement step. The major challenge in designing subdivision schemes thus consists in finding a suitable trade-off between the locality of the subdivision rules and the visual quality of the resulting limit surface.

Focusing on the class of quad-based interpolatory subdivision schemes generalizing the tensor-product version of the Dubuc–Deslauriers 4-point scheme, we can find proposals featured by edge-point rules that either involve $2N + 2$ vertices from the coarser mesh or only a subset of $N + 2$ of them. The existing schemes falling into the first group (see Kobbelt, 1996; Li and Ma, 2007; Li and Zheng, 2012), besides more computationally expensive, are C^1-smooth with unbounded curvature at extraordinary points. As a matter of fact, dealing with refinement rules of larger size not only increases the computational costs for generating the limit surface, but remarkably complicates the tuning of the weights appearing in the affine combination such that bounded curvature at extraordinary points is hardly satisfied. In light of this, we believe strategic to restrict our attention to the subclass of interpolatory subdivision schemes for closed quadrilateral meshes that compute

(i) new edge-points near extraordinary vertices of valence N by means of an affine combination of $N + 2$ vertices from the coarser mesh;

(ii) new face-points near extraordinary vertices of valence N by means of an affine combination of $2N+8$ vertices from the coarser mesh.

Due to requirement (i), the rule for positioning a new vertex on an edge relies only on edge adjacent vertices and not on face adjacent vertices (see Fig. 2). This assumption not only allows the algorithm to reduce the computational costs for generating the limit surface, but reveals that the subdivision scheme can also be thought of as a subdivision scheme for curve networks (Schaefer and Warren, 2003). To the best of our knowledge, the only existing interpolatory subdivision schemes with the property that the position of new edge points is determined exclusively by edge adjacent vertices, are the ones proposed by Schaefer and Warren (2003), Li et al. (2005) and Deng and Ma (2013). All such schemes have been shown independently by their authors to be suitable for generating limit surfaces that are globally C^1 continuous, but while the two most recent ones (namely Li et al., 2005; Deng and Ma, 2013) have also both principal curvatures bounded at extraordinary points, that is not the case for their precursor in Schaefer and Warren (2003). The goal of this article thus consists in identifying the constraints that the weights involved in the edge-point and face-point stencils are required to meet to obtain limit surfaces that are C^1 continuous at extraordinary points with both principal curvatures bounded and at least one of them nonzero.

The remainder of this article consists of six sections. In Section 2 we describe the edge-point and face-point rules characterizing the class of interpolatory subdivision schemes discussed in this work. For such schemes, in Section 3 we construct the local subdivision matrix providing a compact representation of a single refinement step in the vicinity of an extraordinary vertex of valence N, and in Section 4 we derive the explicit formulation of the associated characteristic polynomial and all its roots. In Section 5, we first recall some known results from the literature and then we derive which conditions have to be satisfied by the weights of the extraordinary rules to guarantee C^1 smoothness of the limit surface and boundedness of curvature at extraordinary points. Finally, in Section 6 we exploit the derived conditions to easily check these features in the limit surfaces obtained by the application of special extraordinary rules recently proposed in the literature. We also show that the obtained constraints can be used to design new extraordinary rules able to produce limit surfaces of the same quality as the existing proposals, but at a reduced computational cost. Conclusions are drawn in Section 7.

2. Edge-point and face-point rules

We consider an interpolatory subdivision scheme on quadrilateral meshes generalizing the tensor-product of the 4-point Dubuc–Deslauriers scheme (Deslauriers and Dubuc, 1989; Dubuc, 1986). This means that, when the mesh is regular, that is each vertex has valence $N=4$, the rule for computing the edge-point E_4 is nothing but the 4-point scheme applied to the vertices P_{-1}, P_1, P_0, P_5 (see Fig. 1), i.e.

$$E_4 = -\frac{1}{16}P_{-1} + \frac{9}{16}P_1 + \frac{9}{16}P_0 - \frac{1}{16}P_5, \tag{2.1}$$

while the rule for computing the face-point F_4 is exactly the tensor-product of the edge-point rule, namely

$$\begin{aligned} F_4 = {} & \frac{1}{256}\big(P_{-3}+P_{-8}+P_{-6}+P_6\big) + \frac{81}{256}\big(P_0+P_1+P_2+P_3\big) \\ & - \frac{9}{256}\big(P_{-1}+P_{-2}+P_{-4}+P_{-5}+P_4+P_5+P_7+P_8\big). \end{aligned} \tag{2.2}$$

On the other hand, for meshes of arbitrary manifold topology, special edge-point and face-point rules are defined in the vicinity of extraordinary vertices of valence $N \neq 4$. This work deals with subdivision schemes that apply an $(N+2)$-point and a $(2N+8)$-point stencil respectively for computing edge- and face-points in the neighborhood of an extraordinary vertex of valence $N \neq 4$ (see Fig. 2). More precisely, the edge-point rule used in presence of an extraordinary vertex P_0 of valence $N=3$ is

$$E_3 = -\frac{1}{16}P_{-1} + \frac{9}{16}P_0 + \alpha_{1,3}P_1 + \alpha_{3,3}P_3 + \alpha_{5,3}P_5, \tag{2.3}$$

with $\alpha_{1,3}, \alpha_{3,3}, \alpha_{5,3} \in \mathbb{R}$, while the general edge-point rule to be used when P_0 has valence $N \geq 5$ reads as

$$E_N = -\frac{1}{16}P_{-1} + \frac{9}{16}P_0 + \sum_{j=1}^{N} \alpha_{2j-1,N} P_{2j-1} \tag{2.4}$$

with $\alpha_{2j-1,N} \in \mathbb{R}$ for all $j = 1, \ldots, N$. Thus for all $N \neq 4$ the edge-point rule is defined by an affine combination involving P_{-1}, P_0 and all vertices connected to P_0 by an edge. Analogously, for the face-point rule we consider an affine combination of the four vertices identifying the face of insertion (i.e., P_0, P_1, P_2, P_3) plus the first ring of vertices around it. In formulas, the face-point rule for the case $N=3$ is given by

$$F_3 = \frac{1}{256}(P_{-3} + P_{-6} + P_7) + \frac{81}{256}P_0 - \frac{9}{256}(P_{-1} + P_{-2} + P_{-4} + P_{-5}) + \beta_{1,3}P_1 + \beta_{3,3}P_3 + \beta_{5,3}P_5 + \gamma_{2,3}P_2 + \gamma_{4,3}P_4 + \gamma_{6,3}P_6, \tag{2.5}$$

with $\beta_{1,3}, \beta_{3,3}, \beta_{5,3} \in \mathbb{R}$ and $\gamma_{2,3}, \gamma_{4,3}, \gamma_{6,3} \in \mathbb{R}$, while for the general case $N \geq 5$ it reads as

$$F_N = \frac{1}{256}(P_{-3} + P_{-6} + P_{-2N}) + \frac{81}{256}P_0 - \frac{9}{256}(P_{-1} + P_{-2} + P_{-4} + P_{-5}) + \sum_{j=1}^{N}\beta_{2j-1,N}P_{2j-1} + \sum_{j=1}^{N}\gamma_{2j,N}P_{2j} \tag{2.6}$$

with $\beta_{2j-1,N}, \gamma_{2j,N} \in \mathbb{R}$ for all $j = 1, \ldots, N$. In order to guarantee the symmetry of the scheme and a good visual quality of the limit surface we require the above coefficients to be such that

$$|\alpha_{1,N}| > |\alpha_{2j-1,N}|, \quad j = 2, \ldots, N,$$
$$|\beta_{1,N}| = |\beta_{3,N}| > |\beta_{5,N}| = |\beta_{2N-1,N}| > |\beta_{2j-1,N}|, \quad j = 4, \ldots, N-1,$$
$$|\gamma_{2,N}| > |\gamma_{4,N}| = |\gamma_{2N,N}| > |\gamma_{2j,N}|, \quad j = 3, \ldots, N-1.$$

Taking into account that the regular rules in (2.1)–(2.2) are well-known to generate C^1 limit surfaces (see Deslauriers and Dubuc, 1989; Dubuc, 1986), the goal of this work is to identify the conditions that the free parameters involved in the extraordinary rules have to satisfy in order to guarantee C^1 smoothness also at extraordinary points. To this end, we start by considering the necessary conditions for convergence, inferred by the requirement that the weights of the edge- and face-point stencils sum up to 1 (Peters and Reif, 2008).

Condition 1.a. *For all $N \neq 4$ the necessary conditions for convergence can be shortly written as*

$$A_0^N = \frac{1}{2} \qquad \textit{and} \qquad B_0^N + C_0^N = \frac{13}{16}$$

by introducing the auxiliary notation

$$A_0^N := \sum_{j=1}^{N}\alpha_{2j-1,N}, \qquad B_0^N := \sum_{j=1}^{N}\beta_{2j-1,N}, \qquad C_0^N := \sum_{j=1}^{N}\gamma_{2j,N}. \tag{2.7}$$

3. The local subdivision matrix

By ordering the points counterclockwise along every ring of each sector proceeding outwards from the extraordinary vertex and labeling compatibly within the sectors, the subdivision rules in (2.1)–(2.2) and (2.4)–(2.6) allow one to construct a local subdivision matrix $\mathbf{S}^{[N]} \in \mathbb{R}^{(6N+1)\times(6N+1)}$ of the form

$$\mathbf{S}^{[N]} = \left(\begin{array}{c|c|c|c|c|c} 1 & \mathbf{0} & \mathbf{0} & \cdots & \mathbf{0} & \mathbf{0} \\ \hline \mathbf{w} & \mathbf{M}_0 & \mathbf{M}_1 & \cdots & \mathbf{M}_{N-2} & \mathbf{M}_{N-1} \\ \hline \mathbf{w} & \mathbf{M}_{N-1} & \mathbf{M}_0 & \mathbf{M}_1 & \cdots & \mathbf{M}_{N-2} \\ \hline \mathbf{w} & \mathbf{M}_{N-2} & \ddots & \ddots & \ddots & \vdots \\ \hline \vdots & \vdots & \ddots & \ddots & \ddots & \mathbf{M}_1 \\ \hline \mathbf{w} & \mathbf{M}_1 & \cdots & \mathbf{M}_{N-2} & \mathbf{M}_{N-1} & \mathbf{M}_0 \end{array}\right)$$

where $\mathbf{0} = (0, 0, 0, 0, 0, 0)$, $\mathbf{w} = (\frac{9}{16}, \frac{81}{256}, 0, 0, 0, 0)^T$ and

$$\mathbf{M}_0 = \begin{pmatrix} \alpha_{1,N} & 0 & -\frac{1}{16} & 0 & 0 & 0 \\ \beta_{1,N} & \gamma_{2,N} & -\frac{9}{256} & -\frac{9}{256} & \frac{1}{256} & -\frac{9}{256} \\ 1 & 0 & 0 & 0 & 0 & 0 \\ \frac{9}{16} & \frac{9}{16} & 0 & 0 & 0 & -\frac{1}{16} \\ 0 & 1 & 0 & 0 & 0 & 0 \\ 0 & \frac{9}{16} & 0 & -\frac{1}{16} & 0 & 0 \end{pmatrix}, \qquad \mathbf{M}_1 = \begin{pmatrix} \alpha_{3,N} & 0 & 0 & 0 & 0 & 0 \\ \beta_{3,N} & \gamma_{4,N} & -\frac{9}{256} & \frac{1}{256} & 0 & 0 \\ 0 & 0 & 0 & 0 & 0 & 0 \\ 0 & 0 & 0 & 0 & 0 & 0 \\ 0 & 0 & 0 & 0 & 0 & 0 \\ \frac{9}{16} & -\frac{1}{16} & 0 & 0 & 0 & 0 \end{pmatrix},$$

$$\mathbf{M}_i = \begin{pmatrix} \alpha_{2i+1,N} & 0 & 0 & 0 & 0 & 0 \\ \beta_{2i+1,N} & \gamma_{2i+2,N} & 0 & 0 & 0 & 0 \\ 0 & 0 & 0 & 0 & 0 & 0 \\ 0 & 0 & 0 & 0 & 0 & 0 \\ 0 & 0 & 0 & 0 & 0 & 0 \\ 0 & 0 & 0 & 0 & 0 & 0 \end{pmatrix}, \; i = 2, \dots, N-2, \qquad \mathbf{M}_{N-1} = \begin{pmatrix} \alpha_{2N-1,N} & 0 & 0 & 0 & 0 & 0 \\ \beta_{2N-1,N} & \gamma_{2N,N} & 0 & 0 & 0 & \frac{1}{256} \\ 0 & 0 & 0 & 0 & 0 & 0 \\ 0 & -\frac{1}{16} & 0 & 0 & 0 & 0 \\ 0 & 0 & 0 & 0 & 0 & 0 \\ 0 & 0 & 0 & 0 & 0 & 0 \end{pmatrix}.$$

$\mathbf{S}^{[N]}$ thus provides a compact representation of a single refinement step restricted to the vertices within the 2-ring of an extraordinary vertex P_0 of valence $N \geq 5$. Introducing the notation

$$\mathbf{R}_j := \begin{pmatrix} \frac{1}{N} & 0 \\ \frac{\mathbf{w}}{N} & \mathbf{M}_j \end{pmatrix} \in \mathbb{R}^{7\times 7}, \quad j = 0, \dots, N-1,$$

we construct the $N \times N$ block-circulant matrix

$$\mathbf{R}^{[N]} = \begin{pmatrix} \mathbf{R}_0 & \mathbf{R}_1 & \cdots & \mathbf{R}_{N-2} & \mathbf{R}_{N-1} \\ \mathbf{R}_{N-1} & \mathbf{R}_0 & \mathbf{R}_1 & \cdots & \mathbf{R}_{N-2} \\ \mathbf{R}_{N-2} & \ddots & \ddots & \ddots & \vdots \\ \vdots & \ddots & \ddots & \ddots & \mathbf{R}_1 \\ \mathbf{R}_1 & \cdots & \mathbf{R}_{N-2} & \mathbf{R}_{N-1} & \mathbf{R}_0 \end{pmatrix},$$

and applying a discrete Fourier transform to the blocks $\mathbf{R}_j$, $j = 0, \dots, N-1$, we obtain the blocks

$$\hat{\mathbf{S}}_\nu = \sum_{j=0}^{N-1} \mathbf{R}_j \omega^{j\nu}, \quad \nu = 0, \dots, N-1 \quad \text{with} \quad \omega = e^{\frac{2\pi \mathrm{i}}{N}},$$

defining the block-diagonal matrix

$$\hat{\mathbf{S}}^{[N]} = \begin{pmatrix} \hat{\mathbf{S}}_0 & 0 & \cdots & 0 & 0 \\ 0 & \hat{\mathbf{S}}_1 & 0 & \cdots & 0 \\ \vdots & \ddots & \ddots & \ddots & \vdots \\ 0 & \cdots & 0 & \hat{\mathbf{S}}_{N-2} & 0 \\ 0 & \cdots & 0 & 0 & \hat{\mathbf{S}}_{N-1} \end{pmatrix} \in \mathbb{R}^{7N\times 7N}$$

for which $N-1$ eigenvalues are zero and all the others are exactly the eigenvalues of $\mathbf{S}^{[N]}$. For each rotational frequency component $\nu = 0, \dots, N-1$ the general block $\hat{\mathbf{S}}_\nu \in \mathbb{R}^{7\times 7}$ is of the form

$$\hat{\mathbf{S}}_\nu = \begin{pmatrix} w^N_{0,\nu} & 0 & 0 & 0 & 0 & 0 & 0 \\ w^N_{1,\nu} & A^N_\nu & 0 & -\frac{1}{16} & 0 & 0 & 0 \\ w^N_{2,\nu} & B^N_\nu & C^N_\nu & -\frac{9+9\omega^\nu}{256} & \frac{-9+\omega^\nu}{256} & \frac{1}{256} & \frac{-9+\omega^{(N-1)\nu}}{256} \\ 0 & 1 & 0 & 0 & 0 & 0 & 0 \\ 0 & \frac{9}{16} & \frac{9-\omega^{(N-1)\nu}}{16} & 0 & 0 & 0 & -\frac{1}{16} \\ 0 & 0 & 1 & 0 & 0 & 0 & 0 \\ 0 & \frac{9}{16}\omega^\nu & \frac{9-\omega^\nu}{16} & 0 & -\frac{1}{16} & 0 & 0 \end{pmatrix} \tag{3.1}$$

where

$$A^N_\nu := \sum_{j=1}^{N} \alpha_{2j-1,N}\, \omega^{(j-1)\nu}, \qquad B^N_\nu := \sum_{j=1}^{N} \beta_{2j-1,N}\, \omega^{(j-1)\nu}, \qquad C^N_\nu := \sum_{j=1}^{N} \gamma_{2j,N}\, \omega^{(j-1)\nu}, \tag{3.2}$$

and

$$w^N_{0,\nu} := \frac{1}{N}\sum_{j=0}^{N-1} \omega^{j\nu} = \delta_{\nu,0}, \qquad w^N_{1,\nu} := \frac{1}{N}\sum_{j=0}^{N-1} \frac{9}{16}\omega^{j\nu} = \frac{9}{16}\delta_{\nu,0}, \qquad w^N_{2,\nu} := \frac{1}{N}\sum_{j=0}^{N-1} \frac{81}{256}\omega^{j\nu} = \frac{81}{256}\delta_{\nu,0}, \tag{3.3}$$

with $\delta_{\nu,0}$ denoting the Kronecker delta function.

Remark 3.1. Definition (3.2) implies that $A^N_\nu, B^N_\nu, C^N_\nu \in \mathbb{C}$ for $\nu \neq 0$. Indeed, we will show in Subsection 5.2 that choosing $A^N_\nu, C^N_\nu \in \mathbb{R}$ for all $\nu = 0, \dots, N-1$ we can obtain a local subdivision matrix $\mathbf{S}^{[N]}$ with the desired spectrum.

4. The characteristic polynomial

Let λ_j^ν, $j = 0, \dots, 6$ denote the eigenvalues of the matrix $\hat{\mathbf{S}}_\nu$ in (3.1). Furthermore, whenever μ is an eigenvalue of $\hat{\mathbf{S}}_\nu$, we call ν the *Fourier index* of μ and we write $\mathcal{F}(\mu) = \nu$.

The results in Section 3 allow us to write the complete spectrum of the local subdivision matrix $\hat{\mathbf{S}}^{[N]}$ as

$$\Lambda^{[N]} = \bigcup_{\nu=0}^{N-1} \{\lambda_0^\nu, \lambda_1^\nu, \lambda_2^\nu, \lambda_3^\nu, \lambda_4^\nu, \lambda_5^\nu, \lambda_6^\nu\}.$$

Now let $\mathbf{I}_n$ denote the $n \times n$ identity matrix. To work out the explicit expressions of the eigenvalues of each block $\hat{\mathbf{S}}_\nu$ we have to compute the roots of the characteristic polynomial $\det(\hat{\mathbf{S}}_\nu - \lambda \mathbf{I}_7)$. Using Laplace Expansion Theorem we can write

$$\det(\hat{\mathbf{S}}_\nu - \lambda \mathbf{I}_7) = \left(w_{0,\nu}^N - \lambda\right) \cdot \det(\hat{\mathbf{M}}_\nu - \lambda \mathbf{I}_6), \tag{4.1}$$

where $\hat{\mathbf{M}}_\nu$ is the 6×6 sub-matrix of $\hat{\mathbf{S}}_\nu$ given by

$$\hat{\mathbf{M}}_\nu = \begin{pmatrix} A_\nu^N & 0 & -\frac{1}{16} & 0 & 0 & 0 \\ B_\nu^N & C_\nu^N & -\frac{9+9\omega^\nu}{256} & \frac{-9+\omega^\nu}{256} & \frac{1}{256} & \frac{-9+\omega^{(N-1)\nu}}{256} \\ 1 & 0 & 0 & 0 & 0 & 0 \\ \frac{9}{16} & \frac{9-\omega^{(N-1)\nu}}{16} & 0 & 0 & 0 & -\frac{1}{16} \\ 0 & 1 & 0 & 0 & 0 & 0 \\ \frac{9}{16}\omega^\nu & \frac{9-\omega^\nu}{16} & 0 & -\frac{1}{16} & 0 & 0 \end{pmatrix}. \tag{4.2}$$

As a straightforward consequence of the factorization in (4.1) we have that the eigenvalue of the real matrix $\hat{\mathbf{S}}_0$ that firstly emerges is $\lambda_0^0 = w_{0,0}^N = 1$. Thus $\mathcal{F}(1) = 0$. In contrast, for $\nu = 1, \dots, N-1$, we find $\lambda_0^\nu = w_{0,\nu}^N = 0$, so obtaining all $N-1$ zero eigenvalues of $\hat{\mathbf{S}}^{[N]}$. To compute the remaining eigenvalues of the matrix $\hat{\mathbf{S}}_\nu$ (i.e. λ_j^ν, $j = 1, \dots, 6$ in our notation), we have to compute the eigenvalues of its submatrix $\hat{\mathbf{M}}_\nu$, i.e. the roots of the characteristic polynomial $\det(\hat{\mathbf{M}}_\nu - \lambda \mathbf{I}_6)$. For this purpose we consider the permutation matrix

$$\mathbf{P}_{2,3} = \begin{pmatrix} 1 & 0 & 0 & 0 & 0 & 0 \\ 0 & 0 & 1 & 0 & 0 & 0 \\ 0 & 1 & 0 & 0 & 0 & 0 \\ 0 & 0 & 0 & 1 & 0 & 0 \\ 0 & 0 & 0 & 0 & 1 & 0 \\ 0 & 0 & 0 & 0 & 0 & 1 \end{pmatrix}$$

and observe that, applying $\mathbf{P}_{2,3}$ to the left and to the right of $\hat{\mathbf{M}}_\nu$, we get the block-triangular matrix

$$\tilde{\mathbf{M}}_\nu = \mathbf{P}_{2,3} \hat{\mathbf{M}}_\nu \mathbf{P}_{2,3} = \left(\begin{array}{c|c} \mathbf{K}_1 & \mathbf{O} \\ \hline \mathbf{K}_2 & \mathbf{K}_3 \end{array}\right) \tag{4.3}$$

where $\mathbf{O}$ is the 2×2 null matrix, $\mathbf{K}_1 \in \mathbb{R}^{2\times 2}$, $\mathbf{K}_2 \in \mathbb{R}^{4\times 2}$ and $\mathbf{K}_3 \in \mathbb{R}^{4\times 4}$. Hence, the roots of the characteristic polynomial of $\hat{\mathbf{M}}_\nu$ can be more easily found by computing the roots of the characteristic polynomial of $\tilde{\mathbf{M}}_\nu$ since the latter can be conveniently factorized as

$$\det(\tilde{\mathbf{M}}_\nu - \lambda \mathbf{I}_6) = \det(\mathbf{K}_1 - \lambda \mathbf{I}_2) \cdot \det(\mathbf{K}_3 - \lambda \mathbf{I}_4).$$

The six eigenvalues of $\tilde{\mathbf{M}}_\nu$ are indeed the two roots of

$$\det(\mathbf{K}_1 - \lambda \mathbf{I}_2) = \lambda^2 - A_\nu^N \lambda + \tfrac{1}{16},$$

and the four roots of

$$\det(\mathbf{K}_3 - \lambda \mathbf{I}_4) = \lambda^4 - C_\nu^N \lambda^3 + g_\nu \lambda^2 + h_\nu \lambda + \tfrac{1}{2^{16}}$$

where

$$g_\nu := -\frac{3(3\omega^{2\nu} - 22\omega^\nu + 3)}{2^{11}\omega^\nu} = -\frac{3}{2^{10}}\left(3\cos\left(\frac{2\pi\nu}{N}\right) - 11\right)$$

and

$$h_\nu := \frac{-1+18\omega^\nu+256C_\nu^N\omega^{2\nu}-162\omega^{2\nu}+18\omega^{3\nu}-\omega^{4\nu}}{2^{16}\omega^{2\nu}}$$
$$= \frac{1}{2^{15}}\left(128C_\nu^N-80+18\cos\left(\frac{2\pi\nu}{N}\right)-2\cos^2\left(\frac{2\pi\nu}{N}\right)\right).$$

Computing the roots of the quadratic polynomial we find

$$\lambda_1^\nu = \frac{2A_\nu^N+\sqrt{4(A_\nu^N)^2-1}}{4}, \quad \lambda_2^\nu = \frac{2A_\nu^N-\sqrt{4(A_\nu^N)^2-1}}{4}, \tag{4.4}$$

while computing those of the quartic one we get

$$\begin{aligned}
\lambda_3^\nu &= \frac{C_\nu^N}{4}-S_\nu+\frac{1}{2}\sqrt{-4S_\nu^2-2R_\nu+\frac{T_\nu}{S_\nu}}, & \lambda_4^\nu &= \frac{C_\nu^N}{4}-S_\nu-\frac{1}{2}\sqrt{-4S_\nu^2-2R_\nu+\frac{T_\nu}{S_\nu}},\\
\lambda_5^\nu &= \frac{C_\nu^N}{4}+S_\nu+\frac{1}{2}\sqrt{-4S_\nu^2-2R_\nu-\frac{T_\nu}{S_\nu}}, & \lambda_6^\nu &= \frac{C_\nu^N}{4}+S_\nu-\frac{1}{2}\sqrt{-4S_\nu^2-2R_\nu-\frac{T_\nu}{S_\nu}}
\end{aligned} \tag{4.5}$$

where

$$\begin{aligned}
R_\nu &= \frac{8g_\nu-3(C_\nu^N)^2}{8}, & T_\nu &= \frac{-(C_\nu^N)^3+4C_\nu^Ng_\nu+8h_\nu}{8},\\
\Delta_{\nu,0} &= g_\nu^2+3C_\nu^Nh_\nu+\frac{3}{2^{14}}, & \Delta_{\nu,1} &= 2g_\nu^3+9C_\nu^Ng_\nu h_\nu+\frac{27}{2^{16}}(C_\nu^N)^2+27h_\nu^2-\frac{9}{2^{13}}g_\nu,\\
Q_\nu &= \sqrt[3]{\frac{\Delta_{\nu,1}+\sqrt{\Delta_{\nu,1}^2-4\Delta_{\nu,0}^3}}{2}}, & S_\nu &= \frac{1}{2}\sqrt{-\frac{2}{3}R_\nu+\frac{1}{3}\left(Q_\nu+\frac{\Delta_{\nu,0}}{Q_\nu}\right)}.
\end{aligned}$$

Note that since the blocks $\tilde{\mathbf{M}}_\nu$, $\nu=1,\dots,N-1$ come in complex conjugate pairs, i.e. $\tilde{\mathbf{M}}_{N-\nu}=(\tilde{\mathbf{M}}_\nu)^*$, $\nu=1,\dots,N-1$, then λ_j^ν is eigenvalue of $\tilde{\mathbf{M}}_\nu$ if and only if λ_j^ν is eigenvalue of $\tilde{\mathbf{M}}_{N-\nu}$, i.e. $\mathcal{F}(\lambda_j^\nu)=\{\nu,\ N-\nu\}$, $\nu=1,\dots,N-1$.

5. Constraints on the weights of edge- and face-point extraordinary rules

We start by providing a brief summary of known results concerning the analysis of bivariate subdivision schemes at extraordinary points, since they are needed to understand the content of the following subsections. To get more detailed explanations and see the related proofs we refer the reader to Peters and Reif (2008), Reif (1995), Zorin (1997, 2000).

5.1. Known results from the literature

Let λ_i, $i=0,\dots,6N$ denote the eigenvalues of the local subdivision matrix $\mathbf{S}^{[N]}$ sorted in decreasing order of their modulus, and let $\boldsymbol{z}_i$ denote the associated eigenvectors. If all λ_is have magnitude less than 1, except $\lambda_0=1$ which has Fourier index 0 and a single cyclic subspace of size 1 with eigenvector $\boldsymbol{z}_0=\mathbf{1}$, then the subdivision scheme converges (Zorin, 1997). For symmetric subdivision schemes, in order to achieve C^1 smoothness we need to further assume that the ordered eigenvalues of $\mathbf{S}^{[N]}$ satisfy

$$1=\lambda_0>\lambda:=\lambda_1=\lambda_2>|\lambda_3|,\ \ \lambda\in\mathbb{R}^+,\ \ \mathcal{F}(\lambda)=\{1,\ N-1\}, \tag{5.1}$$

i.e. the sub-dominant eigenvalue λ is real and double, and its Fourier indices are 1 and $N-1$. Moreover, to assert that a symmetric subdivision scheme with a double sub-dominant eigenvalue $\mathbb{R}^+\ni\lambda<1$ generates C^1 limit surfaces for almost all initial data, we have also to require that the characteristic map $\boldsymbol{\Psi}$, defined by the two sub-dominant eigenvectors, is regular and injective (see Reif, 1995; Zorin, 2000). Finally, to design a good C^1 scheme with bounded principal curvatures at the extraordinary point, we additionally need

- the sub-dominant eigenvalue to be $\lambda=\frac{1}{2}$;
- the subsub-dominant eigenvalue to be $\eta=\lambda^2$;
- η to be at least triple and $\mathcal{F}(\eta)\supseteq\{0,2,N-2\}$.

In the following we start by analyzing the case of valence $N\geq 5$ and then we focus on the special case $N=3$ (see Subsection 5.4).

5.2. Constraints inferred from eigenvalues analysis

As previously observed in Section 4, 1 is eigenvalue of the local subdivision matrix $\mathbf{S}^{[N]}$ and $\mathcal{F}(1) = 0$. Moreover, in view of Condition 1.a, $\boldsymbol{z}_0 = \mathbf{1}$ is the associated eigenvector. Thus, provided that all remaining eigenvalues of $\mathbf{S}^{[N]}$ are smaller than 1, the subdivision scheme will be convergent. In the following we identify the constraints to be imposed on the weights of the extraordinary rules such that this can happen. Moreover, in order to fulfill also the necessary conditions to obtain a good C^1 scheme, we will require that the sub-dominant eigenvalue is $\frac{1}{2}$, double and such that its Fourier indices are $1, N-1$, as well as that the subsub-dominant eigenvalue is $\frac{1}{4}$, at least triple and such that $0, 2, N-2$ belong to the set of its Fourier indices, as recalled in Subsection 5.1.

As previously emphasized, since $\tilde{\mathbf{M}}_{N-1} = (\tilde{\mathbf{M}}_1)^*$, to identify the conditions regarding the sub-dominant eigenvalue we can simply focus on the case $\nu = 1$. Thus, we select $\nu = 1$ and observe that, if setting $A_1^N = \frac{5}{8}$, from the eigenvalues expressions in (4.4) we can easily get

$$\lambda_1^1 = \frac{2A_1^N + \sqrt{4(A_1^N)^2 - 1}}{4} = \frac{1}{2},$$

as desired, and also

$$\lambda_2^1 = \frac{2A_1^N - \sqrt{4(A_1^N)^2 - 1}}{4} = \frac{1}{8}.$$

Hence, analogously, the setting of $A_{N-1}^N = \frac{5}{8}$ will provide $\lambda_1^{N-1} = \frac{1}{2}$ and $\lambda_2^{N-1} = \frac{1}{8}$.

Condition 2.a. *The constraint*

$$A_1^N = A_{N-1}^N = \frac{5}{8}, \qquad \forall N \geq 5$$

guarantees the existence of the sub-dominant eigenvalue $\lambda = \frac{1}{2}$ *with Fourier index* $\mathcal{F}(\lambda) = \{1, N-1\}$.

Next, we consider $\nu = 0, 2, \ldots, N-2$ and observe that, if setting $A_\nu^N = \frac{1}{2}$, then from Eq. (4.4) we obtain

$$\lambda_1^\nu = \frac{2A_\nu^N + \sqrt{4(A_\nu^N)^2 - 1}}{4} = \frac{1}{4}, \quad \nu = 0, 2, \ldots, N-2$$

as well as

$$\lambda_2^\nu = \frac{2A_\nu^N - \sqrt{4(A_\nu^N)^2 - 1}}{4} = \frac{1}{4}, \quad \nu = 0, 2, \ldots, N-2.$$

Condition 3.a. *The constraint*

$$A_\nu^N = \frac{1}{2}, \qquad \forall\, \nu = 0, 2, \ldots, N-2 \quad \textit{and} \quad N \geq 5,$$

guarantees the existence of the subsub-dominant eigenvalue $\eta = \frac{1}{4}$ *with multiplicity* $m(\eta) = 2N - 4$ *and Fourier index* $\mathcal{F}(\eta) \supseteq \{0, 2, N-2\}$.

Finally, we have to find an additional condition that can guarantee that all other eigenvalues $\lambda_3^\nu, \lambda_4^\nu, \lambda_5^\nu, \lambda_6^\nu$ are such that $|\lambda_j^\nu| \leq \frac{1}{4}$ for all $j = 3, 4, 5, 6$ and $\nu = 0, 1, \ldots, N-1$. Since the explicit expressions of these eigenvalues exclusively depend on C_ν^N, as shown in Eq. (4.5), to achieve our objective we assume C_ν^N to be a function within the family of real functions

$$\begin{aligned} &f_{\nu,\sigma}^N : [-1, 1] \to \mathbb{R} \\ &\cos\left(\tfrac{2\pi\nu}{N}\right) \mapsto \tfrac{25}{64} - \sigma\left(1 + \cos\left(\tfrac{2\pi\nu}{N}\right)\right), \end{aligned} \tag{5.2}$$

whose members are identified by a specific choice of σ.

Fig. 3 shows the behavior of the family members $f_{\nu,\sigma}^N$ for different values of σ. Plotting also the behavior of the eigenvalues $\lambda_3^\nu, \lambda_4^\nu, \lambda_5^\nu, \lambda_6^\nu$, $\nu = 0, 1, \ldots, N-1$, obtained with $C_\nu^N = f_{\nu,\sigma}^N$, $\sigma \in [\frac{13}{2^{10}}, \frac{45}{2^{10}}]$ (see Fig. 4), we can observe that $|\lambda_3^\nu|, |\lambda_4^\nu|, |\lambda_6^\nu|$ are always smaller than $\frac{1}{4}$, while $|\lambda_5^\nu|$ is not greater than $\frac{1}{4}$ only if $C_\nu^N = f_{\nu,\sigma}^N$ with $\sigma \geq \frac{29}{2^{10}}$. Moreover, we notice that $\lambda_5^\nu = \frac{1}{4}$ whenever $\nu = \frac{N}{2}$ since $C_{\frac{N}{2}}^N = f_{\frac{N}{2},\sigma}^N = \frac{25}{64}$ for all $\sigma \geq \frac{29}{2^{10}}$.

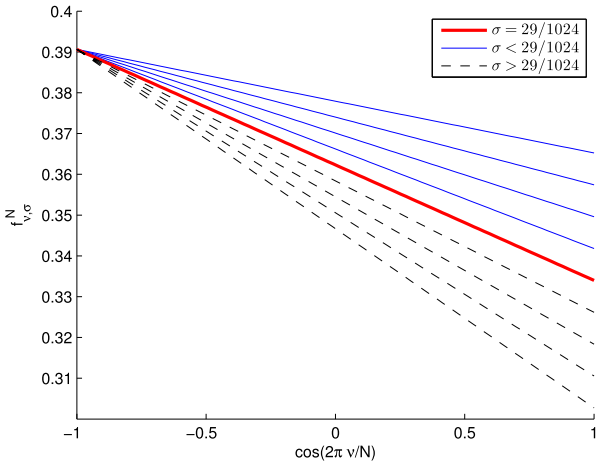

Fig. 3. The family of functions f^N_{ν,σ_i} with $\sigma_i = \frac{13+4i}{2^{10}}$, $i = 0, 1, \ldots, 8$. The solid thicker (red) curve identifies $f^N_{\nu,\frac{29}{2^{10}}}$. (For interpretation of the references to color in this figure legend, the reader is referred to the web version of this article.)

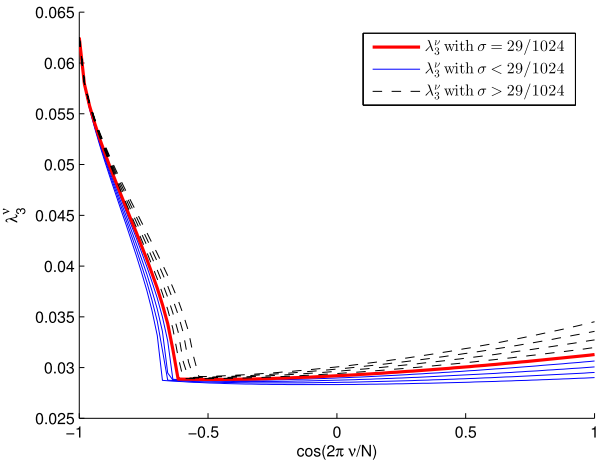

(a) λ^ν_3, $\nu = 0, 1, \ldots, N-1$

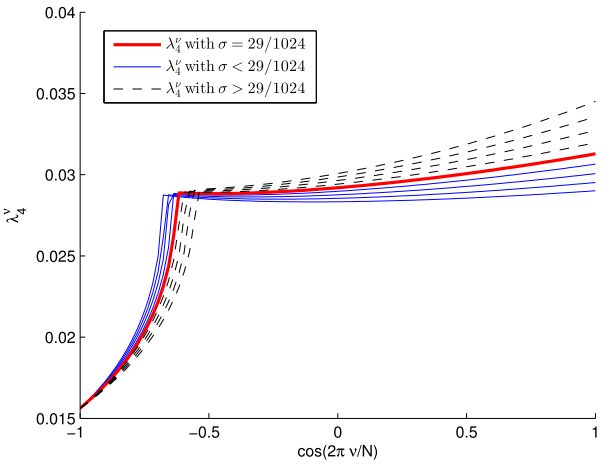

(b) λ^ν_4, $\nu = 0, 1, \ldots, N-1$

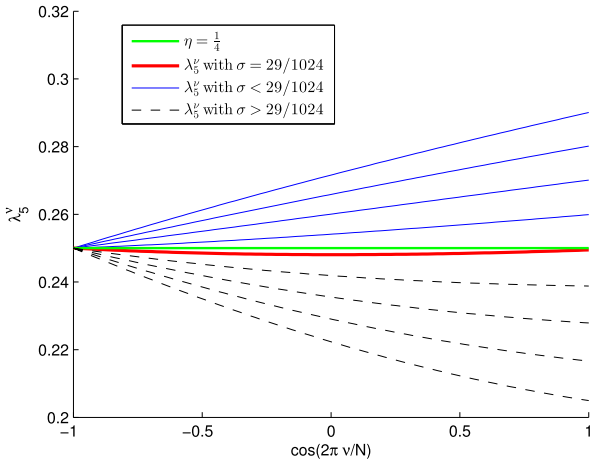

(c) λ^ν_5, $\nu = 0, 1, \ldots, N-1$

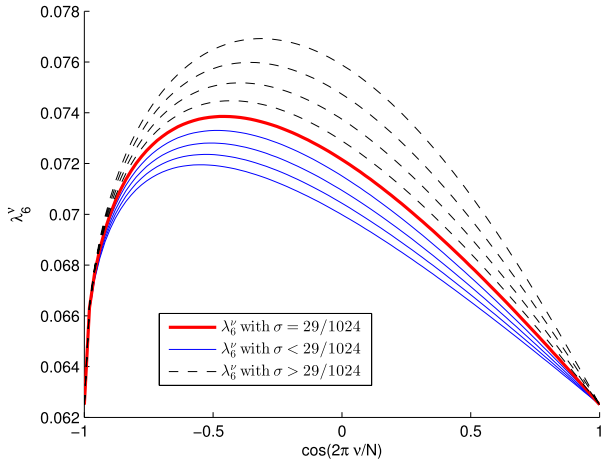

(d) λ^ν_6, $\nu = 0, 1, \ldots, N-1$

Fig. 4. Behavior of eigenvalues $\lambda^\nu_3, \lambda^\nu_4, \lambda^\nu_5, \lambda^\nu_6$, $\nu = 0, 1, \ldots, N-1$ when $C^N_\nu = f^N_{\nu,\sigma_i}$ and $\sigma_i = \frac{13+4i}{2^{10}}$, $i = 0, 1, \ldots, 8$.

Condition 4.a. *Let* $\nu \in \{0, 1, \dots, N-1\}$. *Setting*

$$C_\nu^N = \frac{25}{64} - \sigma\left(1 + \cos\left(\frac{2\pi\nu}{N}\right)\right) \quad \textit{with} \quad \sigma \geq \frac{29}{2^{10}}, \tag{5.3}$$

we obtain

$$|\lambda_3^\nu| < \frac{1}{4}, \quad |\lambda_4^\nu| < \frac{1}{4}, \quad |\lambda_5^\nu| < \frac{1}{4}, \quad |\lambda_6^\nu| < \frac{1}{4}, \quad \textit{if } \nu \neq \frac{N}{2}$$

and

$$|\lambda_3^\nu| < \frac{1}{4}, \quad |\lambda_4^\nu| < \frac{1}{4}, \quad \lambda_5^\nu = \frac{1}{4}, \quad |\lambda_6^\nu| < \frac{1}{4}, \quad \textit{if } \nu = \frac{N}{2}.$$

Remark 5.1. Conditions 3.a and 4.a imply that the subsub-dominant eigenvalue $\eta = \frac{1}{4}$ has multiplicity

$$m(\eta) = \begin{cases} 2N-4, & \text{if } N \text{ odd}, \\ 2N-3, & \text{if } N \text{ even}. \end{cases}$$

Remark 5.2. To guarantee that the local subdivision matrix $\mathbf{S}^{[N]}$ has the desired spectrum, we have no conditions on B_ν^N. Looking at Eqs. (4.2)–(4.3) this can be easily understood. In fact, B_ν^N appears only in the block $\mathbf{K}_2$ which has no influence on the characteristic polynomial and thus on the computation of the eigenvalues of $\tilde{\mathbf{M}}_\nu$.

5.3. Constraints inferred from eigenvectors analysis

If an interpolatory subdivision scheme with extraordinary stencils in Fig. 2 fulfills Conditions 1.a, 2.a, 3.a, 4.a, then it is convergent and satisfies the necessary conditions to achieve also C^1-continuity and bounded curvature at extraordinary points of valence $N \geq 5$. The achievement of C^1-continuity is subject only to the additional fulfillment of the condition regarding the regularity of the characteristic map. In fact, since we already proved that the Fourier indices of the subdominant eigenvalue are $1, N-1$, once the regularity has been proven the injectivity follows immediately (Peters and Reif, 2008). The characteristic map is a special parametrization that allows one to express the limit surface around an extraordinary point as a differentiable function of two variables. Such parametrization depends not only on the mesh connectivity, but also on the weights defining the extraordinary rules, and can be obtained as the planar limit surface generated by the so-called characteristic mesh, i.e. the control mesh provided by the eigenvectors $\boldsymbol{z}_1$, $\boldsymbol{z}_2$ corresponding to the sub-dominant eigenvalue $\lambda := \lambda_1 = \lambda_2$ (Peters and Reif, 2008; Reif, 1995; Zorin, 2000). This planar limit surface is made by a ring of regular surface patches of the tensor-product interpolatory Dubuc–Deslauriers 4-point scheme, and the characteristic mesh contains the control points for the definition of such patches. By the property of rotational symmetry around the extraordinary vertex, the characteristic mesh can be conveniently decomposed into N segments. By normalizing the eigenvectors $\boldsymbol{z}_1$, $\boldsymbol{z}_2$ such that the characteristic mesh is centered at $(0, 0)$ and the furthest corner in the first segment is at $(1, 0)$ of the global (x, y)-coordinate system (see Fig. 5), we can obtain the so-called normalized characteristic mesh. Exploiting the results presented by Deng and Ma (2013, Appendix A), we here show a standard procedure which allows one to verify if a bivariate interpolatory subdivision scheme defined by the extraordinary stencils in Fig. 2 and satisfying Conditions 1.a, 2.a, 3.a, 4.a, has a regular characteristic map, and is thus of class C^1. Before showing the pseudo-code of the procedure, we underline the fact that the eigenvectors $\boldsymbol{z}_1$ and $\boldsymbol{z}_2$, used to define the characteristic mesh, must be computed from a local subdivision matrix $\mathbf{S}^{[N]} \in \mathbb{R}^{(42N+1)\times(42N+1)}$. This is due to the fact that, in the univariate case, for the Dubuc–Deslauriers interpolatory 4-point scheme, a limit curve segment between two consecutive vertices is defined by a set of 6 vertices. For the class of schemes considered in this article, a limit surface patch bounded by 4 vertices defining a quadrilateral face is thus identified by a set of 6×6 vertices, being a tensor-product surface patch of the Dubuc–Deslauriers interpolatory 4-point scheme (see Fig. 5).

Pseudo code of procedure.

1. Compute the subdivision matrix $\mathbf{S}^{[N]} \in \mathbb{R}^{(42N+1)\times(42N+1)}$, where each block $\mathbf{M}_\ell \in \mathbb{R}^{42\times 42}$ for $\ell = 0, 1, \dots, N-1$.
2. Following the reasoning in Section 3, compute the 43×43 block $\hat{\mathbf{S}}_1$ and consider its 42×42 sub-matrix $\hat{\mathbf{M}}_1$.
3. Compute the dominant eigenvector of $\hat{\mathbf{M}}_1$, that is the eigenvector $\mathbf{v} \in \mathbb{C}^{42}$ related to the eigenvalue $\frac{1}{2}$.
4. Re-order the entries $v_k, k = 1, \dots 42$ of $\mathbf{v}$ defining a matrix $\mathbf{V} \in \mathbb{C}^{7\times 6}$ of the form

$$(\mathrm{V}_{i,j})_{\substack{1\leq i\leq 7 \\ 1\leq j\leq 6}} = \begin{pmatrix} v_1 & v_3 & v_7 & v_{13} & v_{21} & v_{31} \\ v_2 & v_4 & v_8 & v_{14} & v_{22} & v_{32} \\ v_6 & v_5 & v_9 & v_{15} & v_{23} & v_{33} \\ v_{12} & v_{11} & v_{10} & v_{16} & v_{24} & v_{34} \\ v_{20} & v_{19} & v_{18} & v_{17} & v_{25} & v_{35} \\ v_{30} & v_{29} & v_{28} & v_{27} & v_{26} & v_{36} \\ v_{42} & v_{41} & v_{40} & v_{39} & v_{38} & v_{37} \end{pmatrix}.$$

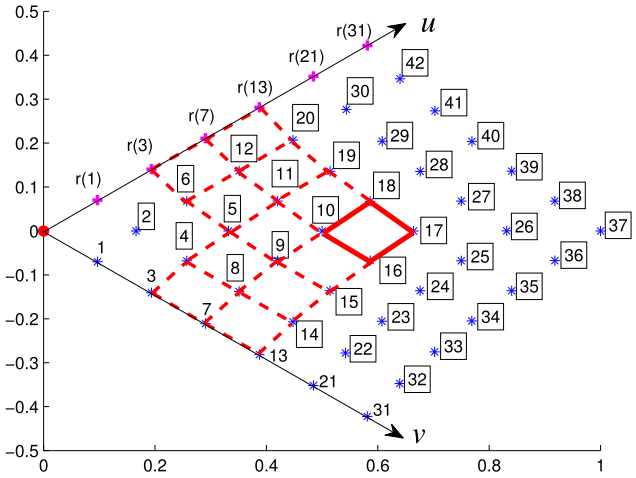

Fig. 5. First segment of the normalized characteristic mesh: entries of the 7×6 matrix $\mathbf{V}$ (marked by $*$) and entries of the first row of $\mathbf{V}$ rotated counterclockwise by $\frac{2\pi}{N}$ (marked by $+$).

5. Denoting by $\boldsymbol{x} := \mathcal{R}(\mathbf{V})$ and $\mathbf{y} := \mathcal{I}(\mathbf{V})$ the real and imaginary part of $\mathbf{V}$, respectively, define the x and y coordinates of the points marked by $*$ in Fig. 5. Notice that they all depend on B_1^N and C_1^N.
6. Rotating rows and columns of $\mathbf{V}$ clockwise and counterclockwise by $\frac{2\pi}{N}$, construct all the 6×6 sets of control points defining the 12 surface patches bounded by the vertices of the quadrilateral faces highlighted in Fig. 5.
7. For the surface patch bounded by the four vertices $\big(\mathcal{R}(\mathrm{V}_{i,j}), \mathcal{I}(\mathrm{V}_{i,j})\big)$, $\big(\mathcal{R}(\mathrm{V}_{i,j+1}), \mathcal{I}(\mathrm{V}_{i,j+1})\big)$, $\big(\mathcal{R}(\mathrm{V}_{i+1,j}), \mathcal{I}(\mathrm{V}_{i+1,j})\big)$, $\big(\mathcal{R}(\mathrm{V}_{i+1,j+1}), \mathcal{I}(\mathrm{V}_{i+1,j+1})\big)$, let $\big(\mathcal{R}(\mathrm{V}_{m,n}) = x_{m,n}, \mathcal{I}(\mathrm{V}_{m,n}) = y_{m,n}\big)$, $m = i-2, \dots, i+3$, $n = j-2, \dots, j+3$ identify its 6×6 set of control points. Then compute

$$
\begin{aligned}
c_m^x &= \max_{n=j-1,\dots,j+2}\{|2x_{m,n} - x_{m,n-1} - x_{m,n+1}|\}, \quad m = i-2, \dots, i+3,\\
\Delta_m^x &= \max\{x_{m+1,j} - x_{m,j},\, x_{m+1,j+1} - x_{m,j+1}\}, \quad m = i-2, \dots, i+2,\\
\delta_m^x &= \min\{x_{m+1,j} - x_{m,j},\, x_{m+1,j+1} - x_{m,j+1}\}, \quad m = i-2, \dots, i+2,
\end{aligned} \tag{5.4}
$$

and verify the fulfillment of

Condition 5.a.

$$
\begin{aligned}
&(i) \quad \frac{(c_{m+1}^x + c_m^x)}{\delta_m^x} < 4 \qquad \forall m = i-2, \dots, i+2,\\
&(ii) \quad \frac{1}{K} \le \frac{4\delta_{m+1}^x - (c_{m+2}^x + c_{m+1}^x)}{4\Delta_m^x + (c_{m+1}^x + c_m^x)} \le K \qquad \forall m = i-2, \dots, i+1,\\
&(iii) \quad \frac{1}{K} \le \frac{4\Delta_{m+1}^x + (c_{m+2}^x + c_{m+1}^x)}{4\delta_m^x - (c_{m+1}^x + c_m^x)} \le K \qquad \forall m = i-2, \dots, i+1,
\end{aligned}
$$

with $K = 3 + 2\sqrt{2}$.

Remark 5.3. Conditions 5.a(i), 5.a(ii), 5.a(iii), together with Conditions 1.a, 2.a, 3.a, 4.a, have been proven by Deng and Ma (2013) to guarantee the positivity of the x and y components of the first derivative of a surface patch along the u direction, and thus, in view of Peters and Reif (2008, Theorem 5.25) provide sufficient conditions for the regularity of the characteristic map.

8. Compute the values in (5.4) for the y-coordinates and check if Condition 5.a is satisfied.
9. Repeat steps 7, 8 for all the 12 surface patches contained in the first sector of the normalized characteristic map.
10. If for all such patches Condition 5.a is verified for both x- and y-coordinates, then the characteristic map is regular. Conversely, if a patch does not satisfy these equations, subdivide it into four subpatches and check Condition 5.a for both x- and y-coordinates of each subpatch. If Condition 5.a is not satisfied within a predefined number of refinement steps (say 10), then no proof of regularity of the characteristic map is available.

Table 1
Weights proposed by Li–Ma–Bao for the edge- and face-point rule around extraordinary vertices of valence $N \geq 5$ (a) and $N = 3$ (b).

(a)

$\alpha_{1,N}$	$\frac{1}{2} + \frac{1}{4N}$
$\alpha_{2j-1,N}, \quad j = 2, \ldots, N$	$\frac{1}{4N} \cos\left(\frac{2\pi(j-1)}{N}\right)$
$\beta_{1,N} = \beta_{3,N}$	$\frac{63}{256} + \frac{3}{32N}\left(2 + \cos\left(\frac{2\pi}{N}\right) + \sin\left(\frac{2\pi}{N}\right)\right)$
$\beta_{5,N} = \beta_{2N-1,N}$	$-\frac{3}{256} + \frac{3}{32N}\left(1 + \cos\left(\frac{4\pi}{N}\right) + \sin\left(\frac{4\pi}{N}\right) + \cos\left(\frac{2\pi}{N}\right) - \sin\left(\frac{2\pi}{N}\right)\right)$
$\beta_{2j-1,N} \quad j = 4, \ldots, N-1$	$\frac{3}{32N}\left(1 + \cos\left(\frac{2\pi(j-1)}{N}\right) + \sin\left(\frac{2\pi(j-1)}{N}\right) + \cos\left(\frac{2\pi(j-2)}{N}\right) - \sin\left(\frac{2\pi(j-2)}{N}\right)\right)$
$\gamma_{2,N}$	$\frac{11}{32} - \frac{7}{64N}$
$\gamma_{4,N} = \gamma_{2N,N}$	$-\frac{3}{128} - \frac{1}{64N}\left(3 + 4\cos\left(\frac{2\pi}{N}\right)\right)$
$\gamma_{2j,N}, \quad j = 3, \ldots, N-1$	$-\frac{1}{64N}\left(3 + 4\cos\left(\frac{2\pi(j-1)}{N}\right)\right)$

(b)

$\alpha_{1,3} = \frac{7}{12}$	$\alpha_{3,3} = \alpha_{5,3} = -\frac{1}{24}$
$\beta_{1,3} = \beta_{3,3} = \frac{75}{256} + \frac{\sqrt{3}}{64}$	$\beta_{5,3} = -\frac{3}{128} - \frac{\sqrt{3}}{32}$
$\gamma_{2,3} = \frac{59}{192}$	$\gamma_{4,3} = \gamma_{6,3} = -\frac{11}{384}$

5.4. The case $N = 3$

The analysis conducted for the case $N \geq 5$ can be exploited also for the special case $N = 3$, just introducing the following changes when formulating Conditions 1.a, 2.a, 3.a and 4.a.

Condition 1.b. *The constraints* $A_0^3 = \frac{1}{2}$, $B_0^3 + C_0^3 = \frac{13}{16}$ *imply that* $\lambda_0 = 1$ *with* $\mathcal{F}(1) = 0$ *and* $\boldsymbol{z}_0 = \mathbf{1}$.

Condition 2.b. *The constraints* $A_1^3 = A_2^3 = \frac{5}{8}$ *imply that* $\lambda := \lambda_1 = \lambda_2 = \frac{1}{2}$ *with* $\mathcal{F}(\lambda) = \{1, 2\}$.

Condition 3.b. *The constraint* $A_0^3 = \frac{1}{2}$ *yields* $\eta := \lambda_3 = \frac{1}{4}$ *with* $\mathcal{F}(\eta) = \{0\}$.

Remark 5.4. We thus point out that, when $N = 3$, the limit surface is not L^2-hyperbolic because both 2 and $N - 2$ do not belong to the Fourier indices of the subsub-dominant eigenvalue $\frac{1}{4}$ (Peters and Reif, 2008).

Condition 4.b. *The constraint* $C_\nu^3 = \frac{25}{64} - \sigma(1 + \cos(\frac{2\pi\nu}{N}))$ *with* $\sigma \geq \frac{29}{2^{10}}$ *for all* $\nu \in \{0, 1, 2\}$ *guarantees that* $|\lambda_i| < \frac{1}{4}$ *for all* $i \geq 4$.

Finally, to check the regularity of the characteristic map, and thus the C^1-continuity of the scheme in the neighborhood of an extraordinary point of valence $N = 3$, we can again use the procedure proposed in Subsection 5.3.

6. Numerical examples: special weights settings

In this section, we consider interpolatory subdivision schemes from the literature which fall into the general class studied in this paper. Such schemes are featured by

(i) the regular rules in (2.1)–(2.2), obtained from the tensor-product of the Dubuc–Deslauriers interpolatory 4-point scheme (Deslauriers and Dubuc, 1989; Dubuc, 1986);
(ii) the extraordinary rules in (2.4)–(2.6) and (2.3)–(2.5) for the cases $N \geq 5$ and $N = 3$, respectively.

Moreover, they satisfy the constraints appearing in Conditions 1.a, 2.a, 3.a, 4.a and 5.a for any $N \neq 4$, and thus guarantee convergence, C^1-continuity and boundedness of principal curvatures at extraordinary points. We thus exclude from our discussion the proposal in Schaefer and Warren (2003) since, although fulfilling requirements (i)–(ii), it fails to satisfy boundedness of curvature.

6.1. Li–Ma–Bao's subdivision scheme

The weights $\alpha_{2j-1,N}, \beta_{2j-1,N}, \gamma_{2j,N}$, $j = 1, \ldots, N$ for the extraordinary rules proposed by Li et al. (2005) are shown in Table 1 for the cases $N \geq 5$ and $N = 3$, respectively. For such weights setting we prove that the constraints in Conditions 1.a, 2.a, 3.a, 4.a are all satisfied for any $N \neq 4$.

Proposition 6.1. *Li–Ma–Bao's subdivision scheme satisfies the constraints in Condition 1.a for all* $N \geq 5$.

Proof. From Table 1a we have that

$$A_0^N = \sum_{j=1}^{N} \alpha_{2j-1,N} = \frac{1}{2} + \frac{1}{4N} + \frac{1}{4N} \sum_{j=2}^{N} \cos\left(\frac{2\pi(j-1)}{N}\right).$$

Since $\sum_{j=2}^{N} \cos\left(\frac{2\pi(j-1)}{N}\right) = -1$ for all $N \geq 5$, then $A_0^N = \frac{1}{2}$. In order to compute B_0^N, we observe that

$$\frac{3}{32N} \sum_{j=1}^{N} \left(1 + \cos\left(\frac{2\pi(j-1)}{N}\right) + \sin\left(\frac{2\pi(j-1)}{N}\right) + \cos\left(\frac{2\pi(j-2)}{N}\right) - \sin\left(\frac{2\pi(j-2)}{N}\right)\right) = \frac{3}{32} \quad \forall N \geq 5,$$

and the latter yields $B_0^N = \frac{3}{32} + 2 \cdot \frac{63}{256} + 2 \cdot \left(-\frac{3}{256}\right) = \frac{9}{16}$. In a similar way we can compute C_0^N by noticing that

$$-\frac{1}{64N} \sum_{j=1}^{N} \left(3 + 4\cos\left(\frac{2\pi(j-1)}{N}\right)\right) = -\frac{3}{64} \quad \forall N \geq 5,$$

which yields $C_0^N = -\frac{3}{64} + \frac{11}{32} + 2 \cdot \left(-\frac{3}{128}\right) = \frac{1}{4}$. Hence $B_0^N + C_0^N = \frac{13}{16}$. □

For the following propositions we recall that $\omega = e^{\frac{2\pi i}{N}} = \cos\left(\frac{2\pi}{N}\right) + i\sin\left(\frac{2\pi}{N}\right)$.

Proposition 6.2. *Li–Ma–Bao's subdivision scheme satisfies the constraints in Condition 2.a for all $N \geq 5$.*

Proof. Since

$$\frac{1}{4N} \sum_{j=1}^{N} \cos\left(\frac{2\pi(j-1)}{N}\right) \omega^{(j-1)} = \frac{1}{8} \qquad \forall N \geq 5,$$

thus $A_1^N = \frac{1}{8} + \frac{1}{2} = \frac{5}{8}$ for all $N \geq 5$. Analogously we can also prove that $A_{N-1}^N = \frac{5}{8}$ for all $N \geq 5$. □

Proposition 6.3. *Li–Ma–Bao's subdivision scheme satisfies the constraints in Condition 3.a for all $N \geq 5$.*

Proof. In Proposition 6.1 we have already proven that $A_0^N = \frac{1}{2}$. Thus, we have to prove the claim for $\nu = 2, \ldots, N-2$ only. Since for all $N \geq 5$ and $\nu = 2, \ldots, N-2$

$$\frac{1}{4N} \sum_{j=1}^{N} \cos\left(\frac{2\pi(j-1)}{N}\right) \omega^{(j-1)\nu} = 0,$$

then $A_\nu^N = \frac{1}{2}$ for all $N \geq 5$ and $\nu = 2, \ldots, N-2$. □

Proposition 6.4. *Li–Ma–Bao's subdivision scheme satisfies the constraints in Condition 4.a for all $N \geq 5$.*

Proof. Using the coefficients in Table 1a we can compute C_ν^N for all $\nu = 0, \ldots, N-1$.

- If $\nu = 0$, then $C_0^N = \frac{1}{4}$ as it was already shown in Proposition 6.1.
- If $\nu = 1$, we observe that for all $N \geq 5$

$$-\frac{1}{64N} \sum_{j=1}^{N} \left(3 + 4\cos\left(\frac{2\pi(j-1)}{N}\right)\right) \omega^{(j-1)} = -\frac{1}{32},$$

so that

$$C_1^N = \frac{5}{16} - \frac{3}{128}\left(\omega + \omega^{N-1}\right) \qquad \forall\ N \geq 5.$$

Analogously, we can also show that $C_{N-1}^N = \frac{5}{16} - \frac{3}{128}\left(\omega + \omega^{N-1}\right)$, for all $N \geq 5$.

Table 2
Weights proposed by Deng–Ma for the edge- and face-point rule around extraordinary vertices of valence $N \geq 5$ (a) and $N = 3$ (b).

(a)

$\alpha_{1,N}$	$\frac{1}{2} + \frac{1}{4N}$
$\alpha_{2j-1,N}, \quad j = 2, \ldots, N$	$\frac{1}{4N} \cos\left(\frac{2\pi(j-1)}{N}\right)$
$\beta_{1,N} = \beta_{3,N}$	$\frac{153}{512} + \frac{9}{128N}\left(1 + \cos\left(\frac{2\pi}{N}\right)\right)$
$\beta_{5,N} = \beta_{2N-1,N}$	$-\frac{9}{512} + \frac{9}{128N}\left(\cos\left(\frac{4\pi}{N}\right) + \cos\left(\frac{2\pi}{N}\right)\right)$
$\beta_{2j-1,N}, \quad j = 4, \ldots, N-1$	$\frac{9}{128N}\left(\cos\left(\frac{2\pi(j-1)}{N}\right) + \cos\left(\frac{2\pi(j-2)}{N}\right)\right)$
$\gamma_{2,N}$	$\frac{81}{256}$
$\gamma_{4,N} = \gamma_{2N,N}$	$-\frac{9}{256}$
$\gamma_{6,N} = \gamma_{2N-2,N}$	$\frac{1}{512}$
$\gamma_{2j,N}, \quad j = 4, \ldots, N-2$	0

(b)

$\alpha_{1,3} = \frac{7}{12}$	$\alpha_{3,3} = \alpha_{5,3} = -\frac{1}{24}$
$\beta_{1,3} = \beta_{3,3} = \frac{159}{512}$	$\beta_{5,3} = -\frac{15}{256}$
$\gamma_{2,3} = \frac{81}{256}$	$\gamma_{4,3} = \gamma_{6,3} = -\frac{17}{512}$

- If $\nu = 2, \ldots, N-2$, we notice that for all $N \geq 5$

$$-\frac{1}{64N} \sum_{j=1}^{N} \left(3 + 4\cos\left(\frac{2\pi(j-1)}{N}\right)\right) \omega^{(j-1)\nu} = 0,$$

thus yielding

$$C_\nu^N = \frac{11}{32} - \frac{3}{128}\left(\omega^\nu + \omega^{(N-1)\nu}\right) \qquad \forall N \geq 5 \text{ and } \nu = 2, \ldots, N-2.$$

Finally, re-writing the above results in the compact form

$$C_\nu^N = \begin{cases} \frac{1}{4} & \text{if} \quad \nu = 0; \\ \frac{23}{64} - \frac{3}{64}\left(1 + \cos\left(\frac{2\pi}{N}\right)\right) & \text{if} \quad \nu = 1, N-1; \\ \frac{25}{64} - \frac{3}{64}\left(1 + \cos\left(\frac{2\pi\nu}{N}\right)\right) & \text{if} \quad \nu = 2, \ldots, N-2 \end{cases}$$

we get

$$C_\nu^N = \begin{cases} f^N_{0,\frac{9}{128}} & \text{if} \quad \nu = 0; \\ f^N_{1,\frac{3}{64}+\frac{1}{32(1+\cos(\frac{2\pi}{N}))}} & \text{if} \quad \nu = 1, N-1; \\ f^N_{\nu,\frac{3}{64}} & \text{if} \quad \nu = 2, \ldots, N-2. \end{cases}$$

Since $\frac{9}{128} > \frac{29}{2^{10}}$, $\frac{3}{64} > \frac{29}{2^{10}}$ and $\frac{3}{64} + \frac{1}{32(1+\cos(\frac{2\pi}{N}))} > \frac{3}{64} > \frac{29}{2^{10}}$, then for all $0 \leq \nu \leq N-1$ the constraints in Condition 4.a are satisfied. □

Remark 6.5. From Table 1b we obtain that, when $N = 3$, Li–Ma–Bao's scheme satisfies the constraints in Conditions 1.b and 3.b since $A_0^3 = \frac{1}{2}$ and $B_0^3 = \frac{9}{16}$, $C_0^3 = \frac{1}{4}$, so providing $B_0^3 + C_0^3 = \frac{13}{16}$. Additionally, since $A_1^3 = A_2^3 = \frac{7}{12} - \frac{1}{12}\cos\left(\frac{2\pi}{3}\right) = \frac{5}{8}$, the constraints in Condition 2.b are also fulfilled. Furthermore, since $C_0^3 = \frac{1}{4} = f^3_{0,\frac{9}{128}}$ and $C_1^3 = C_2^3 = \frac{43}{128} = f^3_{1,\frac{7}{64}}$ with $\frac{9}{128} > \frac{29}{2^{10}}$ and $\frac{7}{64} > \frac{29}{2^{10}}$, thus the constraints in Condition 4.b are satisfied too for all $0 \leq \nu \leq 2$.

Finally, using the numerical procedure summarized in Subsection 5.3, we checked that Li–Ma–Bao's scheme also satisfies Condition 5.a for all $3 \leq N \leq 50$ after 7 refinement steps, thus showing convergence, C^1-smoothness and boundedness of principal curvatures at extraordinary points with these valences.

6.2. Deng–Ma's subdivision scheme

For the subdivision scheme recently proposed by Deng and Ma (2013), the weights defining the edge-point and the face-point stencil are shown in Table 2 for $N \geq 5$ and $N = 3$. As already shown for Li–Ma–Bao's subdivision scheme, we now prove that also the coefficients defining the extraordinary rules of Deng–Ma's scheme satisfy the constraints in Conditions 1.a, 2.a, 3.a and 4.a.

Remark 6.6. Comparing Tables 1a and 2a, we notice that the coefficients $\alpha_{2j-1,N}$, $j=1,\dots,N$ are the same for both schemes. Thus, Propositions 6.2 and 6.3 immediately yield that Deng–Ma's subdivision scheme satisfies the constraints in Conditions 2.a and 3.a.

Proposition 6.7. *Deng–Ma's subdivision scheme satisfies the constraints in Condition 1.a for all $N \geq 5$.*

Proof. From Remark 6.6 we have that $A_0^N = \frac{1}{2}$. Now, in order to compute B_0^N we observe that, for all $N \geq 5$,

$$\frac{9}{128N}\sum_{j=1}^{N}\left(\cos\left(\frac{2\pi(j-1)}{N}\right)+\cos\left(\frac{2\pi(j-2)}{N}\right)\right)=0,$$

so that $B_0^N = 2\cdot\frac{153}{512}+2\cdot\left(-\frac{9}{512}\right)=\frac{9}{16}$. Additionally, from Table 2a we have that $C_0^N=\frac{1}{4}$ so obtaining $B_0^N+C_0^N=\frac{13}{16}$. □

Proposition 6.8. *Deng–Ma's subdivision scheme satisfies the constraints in Condition 4.a for all $N \geq 5$.*

Proof. From Table 2a we find that, for all $N \geq 5$ and $\nu = 0,\dots,N-1$,

$$C_\nu^N = \frac{81}{256}-\frac{9}{128}\cos\left(\frac{2\pi\nu}{N}\right)+\frac{1}{256}\cos\left(\frac{4\pi\nu}{N}\right)=f^N_{\nu,\frac{10-\cos\left(\frac{2\pi\nu}{N}\right)}{128}} \qquad \text{with} \quad \frac{10-\cos\left(\frac{2\pi\nu}{N}\right)}{128}>\frac{29}{2^{10}}.$$

Then the constraints in Condition 4.a are fulfilled. □

Remark 6.9. From Table 2b we immediately find that $A_0^3=\frac{1}{2}$, $B_0^3=\frac{9}{16}$, $C_0^3=\frac{1}{4}$, so that $B_0^3+C_0^3=\frac{13}{16}$. Hence Deng–Ma's subdivision scheme satisfies the constraints in Conditions 1.b and 3.b. Additionally, since $A_1^3=A_2^3=\frac{7}{12}-\frac{1}{12}\cos\left(\frac{2\pi}{3}\right)=\frac{5}{8}$, the constraints in Condition 2.b are also fulfilled. Furthermore, by the fact that $C_0^3=\frac{1}{4}=f^3_{0,\frac{9}{128}}$, $C_1^3=C_2^3=\frac{179}{512}=f^3_{1,\frac{21}{256}}$ and $\frac{9}{128}>\frac{29}{2^{10}}$ as well as $\frac{21}{256}>\frac{29}{2^{10}}$, thus the constraints in Condition 4.b are satisfied too.

Finally, we conclude by observing that, using the numerical procedure in Subsection 5.3, Deng–Ma's scheme also satisfies Condition 5.a for all $3\leq N\leq 50$ with 8 refinement steps, and thus guarantees convergence, C^1-continuity and boundedness of principal curvatures at extraordinary points with these valences.

6.3. A new scheme with simplified face-point stencils

The goal of this section is to show how easily new C^1 subdivision schemes with bounded curvature at extraordinary points can be designed by suitably choosing the weights $\alpha_{2j-1,N}$, $\beta_{2j-1,N}$, $\gamma_{2j,N}$, $j=1,\dots,N$ such that all the constraints previously found are fulfilled. Keeping the regular rules in (2.1)–(2.2) and the choice of $\alpha_{2j-1,N}$, $j=1,\dots,N$ for all $N\neq 4$ as in Li–Ma–Bao's and Deng–Ma's proposal, we focus our attention on the selection of the weights appearing in the face-point rule only. Our idea is to simplify the expressions of the coefficients used in the above proposals and to reduce the number of vertices involved. To this purpose we choose the weights for the face-point stencil as follows:

- if $N=3$, we set

$$\beta_{1,3}=\beta_{3,3}=\frac{79}{256},\quad \beta_{5,3}=-\frac{19}{256},\qquad \gamma_{2,3}=\frac{85}{256},\quad \gamma_{4,3}=\gamma_{6,3}=-\frac{1}{32}, \tag{6.1}$$

- if $N\geq 5$ we choose

$$\begin{aligned}&\beta_{1,N}=\beta_{3,N}=\frac{81}{256},\quad \beta_{5,N}=\beta_{2N-1,N}=\frac{N-38}{512(N-2)},\quad \beta_{2j-1,N}=-\frac{9}{128(N-2)},\quad j=4,\dots,N-1\\ &\gamma_{2,N}=\frac{81}{256},\quad \gamma_{4,N}=\gamma_{2N,N}=-\frac{9}{256},\quad \gamma_{2j,N}=0,\quad j=3,\dots,N-1.\end{aligned} \tag{6.2}$$

Regarding the new choice of the coefficients $\beta_{2j-1,N}$, $j=1,\dots,N$ we observe that they have a simpler expression than those proposed by Li–Ma–Bao and Deng–Ma. Moreover, the coefficients $\gamma_{2j,N}$, $j=1,\dots,N$ are independent of the valence N and only 3 of them are non-zero. Thus the choice in (6.1)–(6.2) is computationally cheaper since we simplify the expressions of $\beta_{2j-1,N}$ and $\gamma_{2j,N}$, and reduce the number of vertices involved in the face-point rule definition.

In the following we show that the new weights fulfill all the necessary conditions required for C^1-continuity and bounded curvature at extraordinary vertices of valence $N=3$ and $N\geq 5$.

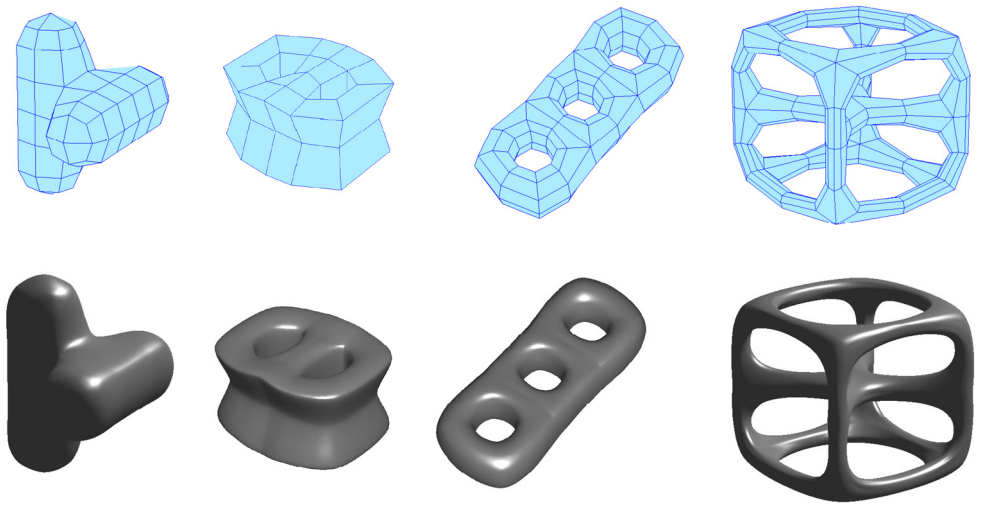

Fig. 6. Limit surfaces obtained by the subdivision scheme proposed in Subsection 6.3 after 6 steps of refinement.

Proposition 6.10. *The interpolatory subdivision scheme with coefficients in (6.1) and (6.2) satisfies Conditions 1.b, 2.b, 3.b, 4.b for valence $N = 3$ and Conditions 1.a, 2.a, 3.a, 4.a for valence $N \geq 5$.*

Proof. Since we keep the same $\alpha_{2j-1,N}$ $j = 1, \ldots, N$ proposed by Li–Ma–Bao and Deng–Ma, from Remarks 6.5 and 6.9 we immediately have that for $N = 3$ Conditions 2.b and 3.b are verified and, in the same way, from Propositions 6.2 and 6.3 we have that for $N \geq 5$ Conditions 2.a and 3.a are fulfilled. Additionally, we can easily see that $B_0^3 + C_0^3 = \frac{13}{16}$, thus satisfying Condition 1.b. For $N \geq 5$ we notice that $\sum_{j=2}^{N-1} \left(-\frac{9}{128(N-2)}\right) = -\frac{9}{128}$. It easily follows that $B_0^N = \frac{145}{256}$ and, since $C_0^N = \frac{63}{256}$, we have $B_0^N + C_0^N = \frac{13}{16}$ and Condition 1.a is verified. Furthermore, by the fact that, for $N = 3$, $C_0^3 = \frac{69}{256} = f^3_{0,\frac{31}{512}}$ and $C_1^3 = C_2^3 = \frac{93}{256} = f^3_{1,\frac{7}{128}}$ where $\frac{31}{512} > \frac{29}{2^{10}}$ as well as $\frac{7}{128} > \frac{29}{2^{10}}$, Condition 4.b is satisfied too. In a similar way, we find

$$C_\nu^N = \frac{81}{256} - \frac{9}{128}\cos\left(\frac{2\pi\nu}{N}\right) = f^N_{\nu,\frac{9}{128}+\frac{1}{256\cos\left(\frac{2\pi\nu}{N}\right)}}$$

and since $\frac{9}{128} + \frac{1}{256\cos\left(\frac{2\pi\nu}{N}\right)} > \frac{29}{2^{10}}$ for all $0 \leq \nu \leq N-1$, then for all $0 \leq \nu \leq N-1$ Condition 4.a is fulfilled. □

Finally, using the numerical procedure in Subsection 5.3, we have verified that the new interpolatory subdivision scheme satisfies Condition 5.a for all $3 \leq N \leq 50$ after 9 refinement steps, and thus guarantees convergence, C^1-continuity and boundedness of principal curvatures at extraordinary points with these valences.

In Fig. 6 we show four examples of initial control meshes refined by using the new interpolatory subdivision scheme. In Fig. 7 we compare the limit surfaces obtained by the new extraordinary rules with the ones obtained via Li–Ma–Bao's and Deng–Ma's proposals. Analyzing the behavior of the reflection lines it turns out that the new scheme produces limit surfaces of the same quality as Deng–Ma's and Li–Ma–Bao's schemes, but at a reduced computational cost.

7. Conclusions

In this work we studied which constraints are required to be respected by the weights of the extraordinary stencils shown in Fig. 2 to obtain a limit surface that is C^1-continuous and with bounded curvature at the extraordinary points. The necessary conditions defined by analyzing the eigenvalues of the subdivision matrix are summarized in Table 3 for all extraordinary points of valence $N \neq 4$. Moreover, a standard procedure that checks sufficient conditions for the regularity of the characteristic map has been presented in Subsection 5.3. These conditions allow one to define a large variety of C^1-interpolatory schemes with bounded curvature. After proving that the schemes proposed in literature by Li–Ma–Bao and Deng–Ma satisfy all the above constraints, we have derived a new subdivision scheme characterized by a smaller and simplified face-point stencil, which behaves closely to Deng–Ma's and Li–Ma–Bao's schemes.

Acknowledgements

This work was partially supported by Italian GNCS-INdAM within the research project entitled "Mathematical and computational models for the representation of complicated geometries" and MIUR-PRIN 2012 (grant No. 2012MTE38N).

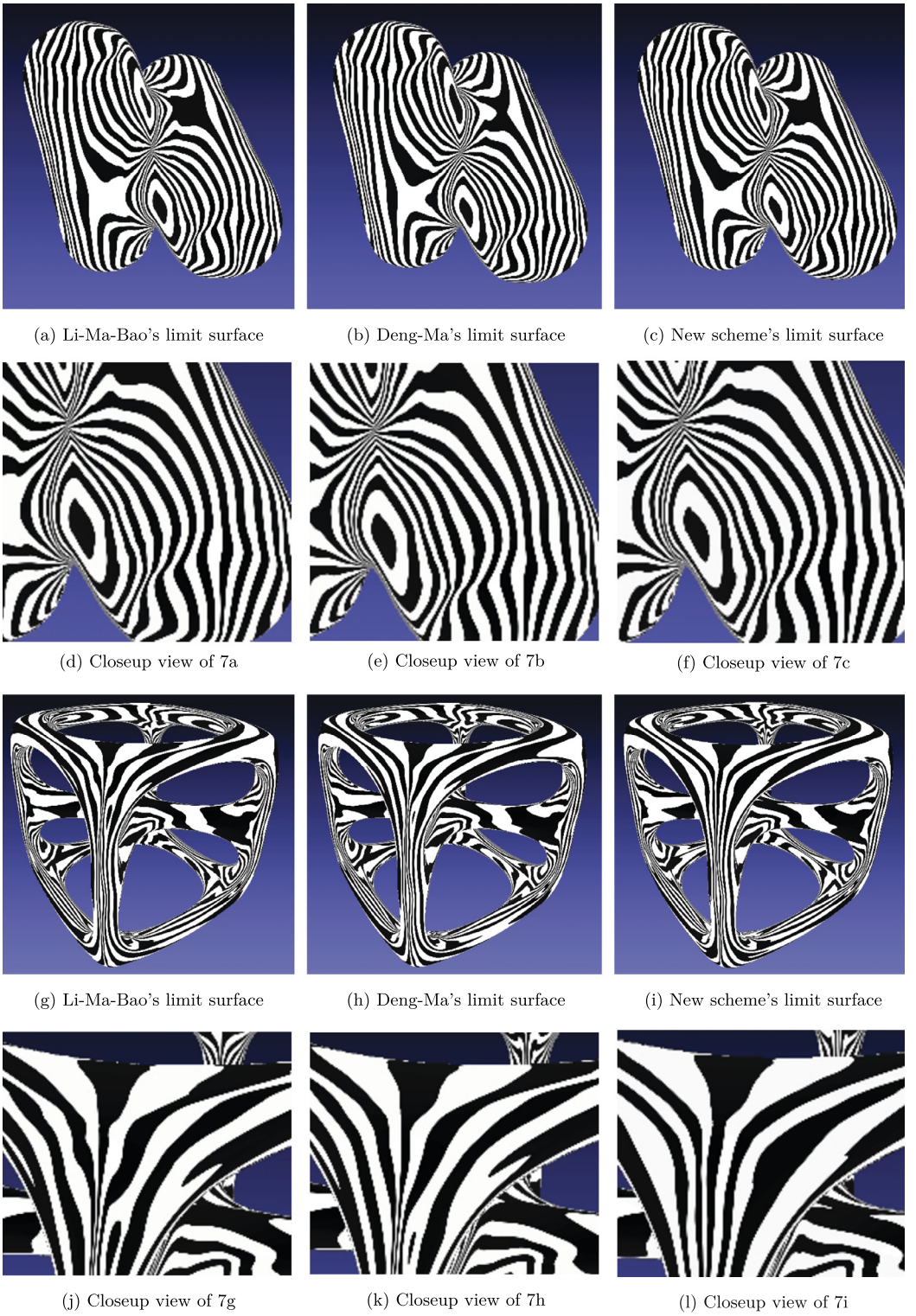

(a) Li-Ma-Bao's limit surface (b) Deng-Ma's limit surface (c) New scheme's limit surface

(d) Closeup view of 7a (e) Closeup view of 7b (f) Closeup view of 7c

(g) Li-Ma-Bao's limit surface (h) Deng-Ma's limit surface (i) New scheme's limit surface

(j) Closeup view of 7g (k) Closeup view of 7h (l) Closeup view of 7i

Fig. 7. First and third row: comparison of C^1 limit surfaces (obtained after 6 steps of refinement) displayed with reflection lines. Second and fourth row: closeup views at extraordinary vertices of valence 3 and 6, respectively.

Table 3
Summary of the conditions required on the coefficients $\alpha_{2j-1,N}$, $\beta_{2j-1,N}$, $\gamma_{2j,N}$, $j = 1, \dots, N$ for all valences $N \neq 4$.

1.	$\sum_{j=1}^{N} \alpha_{2j-1,N} = \frac{1}{2}$ for all $N \neq 4$, $\quad \sum_{j=1}^{N} (\beta_{2j-1,N} + \gamma_{2j,N}) = \frac{13}{16}$ for all $N \neq 4$
2.	$\sum_{j=1}^{N} \alpha_{2j-1,N}\, \omega^{(j-1)\nu} = \frac{5}{8}$ for all $N \neq 4$ and $\nu = 1, N-1$
3.	$\sum_{j=1}^{N} \alpha_{2j-1,N}\, \omega^{(j-1)\nu} = \frac{1}{2}$ for $N \geq 5$ and $\nu = 0, 2, \dots, N-2$
4.	$\sum_{j=1}^{N} \gamma_{2j,N}\, \omega^{(j-1)\nu} = \frac{25}{64} - \sigma \left(1 + \cos\left(\frac{2\pi\nu}{N}\right)\right)$ with $\sigma \geq \frac{29}{2^{10}}$ for all $N \neq 4$ and $\nu = 0, 1, \dots, N-1$

The authors are grateful to Laura Valerio for cooperating in producing the pictures contained in this article and to the anonymous referees for their careful reading of the manuscript.

References

Deng, C., Ma, W., 2013. A unified interpolatory subdivision scheme for quadrilateral meshes. ACM Trans. Graph. 32 (3), 1–11. Article 23.
Deslauriers, G., Dubuc, S., 1989. Symmetric iterative interpolation processes. Constr. Approx. 5 (1), 49–68.
Dubuc, S., 1986. Interpolation through an iterative scheme. J. Math. Anal. Appl. 114 (1), 185–204.
Kobbelt, L., 1996. Interpolatory subdivision on open quadrilateral nets with arbitrary topology. Comput. Graph. Forum: Proceedings of Eurographics 15 (3), 409–420.
Li, G., Ma, W., 2007. A method for constructing interpolatory subdivision schemes and blending subdivisions. Comput. Graph. Forum 26 (2), 185–201.
Li, X., Zheng, J., 2012. An alternative method for constructing interpolatory subdivision from approximating subdivision. Comput. Aided Geom. Des. 29 (7), 474–484.
Li, G., Ma, W., Bao, H., 2005. A new interpolatory subdivision for quadrilateral meshes. Comput. Graph. Forum 24 (1), 3–16.
Peters, J., Reif, U., 2008. Subdivision Surfaces. Springer.
Reif, U., 1995. A unified approach to subdivision algorithms near extraordinary vertices. Comput. Aided Geom. Des. 12, 153–174.
Schaefer, S., Warren, J., 2003. A factored interpolatory subdivision scheme for quadrilateral surfaces. In: Cohen, A., Merrien, J.L., Schumaker, L.L. (Eds.), Curve and Surface Fitting: Saint-Malo, pp. 373–382.
Zorin, D., 1997. Stationary subdivision and multiresolution surface representations. PhD thesis. Caltech, Pasadena, California.
Zorin, D., 2000. A method for analysis of C^1-continuity of subdivision surfaces. SIAM J. Numer. Anal. 35 (5), 1677–1708.